Chapter 8

# INFLUENCE FUNCTIONAL FOR DECOHERENCE OF INTERACTING ELECTRONS IN DISORDERED CONDUCTORS

Jan von Delft
*Sektion Physik und Center for NanoScience der Ludwig-Maximilians-Universität München, Theresienstr. 37, 80333, München, Germany*

**Abstract** We have rederived the controversial influence functional approach of Golubev and Zaikin (GZ) for interacting electrons in disordered metals in a way that allows us to show its equivalence, before disorder averaging, to diagrammatic Keldysh perturbation theory. By representing a certain Pauli factor $(\tilde{\delta} - 2\tilde{\rho}^0)$ occuring in GZ's effective action in the frequency domain (instead of the time domain, as GZ do), we also achieve a more accurate treatment of recoil effects. With this change, GZ's approach reproduces, in a remarkably simple way, the standard, generally accepted result for the decoherence rate.

**Keywords:** Decoherence, influence functional, diagrammatic perturbation theory, interactions, disorder

## 1. Introduction

A few years ago, Golubev and Zaikin (GZ) developed an influence functional approach for describing interacting fermions in a disordered conductor. Their key idea was as follows: to understand how the diffusive behavior of a given electron is affected by its interactions with other electrons in the system, which constitute its effective environment, the latter should be integrated out, leading to an influence functional, denoted by $e^{-(i\tilde{S}_R+\tilde{S}_I)}$, in the path integral $\int \tilde{\mathcal{D}}' \boldsymbol{R}$ describing its dynamics. To derive the effective action $(i\tilde{S}_R + \tilde{S}_I)$, GZ devised a strategy which, when implemented with sufficient care, *properly incorporates the Pauli principle* – this is essential, since both the particle and its environment originate from the same system of indistinghuishable fermions, a feature which

makes the present problem conceptually interesting and sets it apart from all other applications of influence functionals that we are aware of.

GZ used their new approach to calculate the electron decoherence rate $\gamma_\varphi(T)$ in disordered conductors, as extracted from the magnetoconductance in the weak localization regime, and found it to be finite at zero temperature [1, 2, 3, 4, 5, 6], $\gamma_\varphi^{\rm GZ}(T\to 0)=\gamma_\varphi^{0,{\rm GZ}}$, in apparent agreement with some experiments [7]. However, this result contradicts the standard view, based on the work of Altshuler, Aronov and Khmelnitskii (AAK) [9], that $\gamma_\varphi^{\rm AAK}(T\to 0)=0$, and hence elicited a considerable and ongoing controversy [8]. GZ's work was widely questioned, for example in Refs. [10, 11, 12, 13, 14, 15], with the most detailed and vigorous critique coming from Aleiner, Altshuler and Gershenzon (AAG) [16] and Aleiner, Altshuler and Vavilov (AAV) [17, 18], but GZ rejected each critique [3, 4, 5, 8] with equal vigor. It is important to emphasize that the debate here is about a well-defined theoretical model, and not about experiments which do or do not support GZ's claim.

The fact that GZ's final results for $\gamma_\varphi^{\rm GZ}(T)$ have been questioned, however, does not imply that their influence functional approach, as such, is fundamentally flawed. To the contrary, we show in this paper that it is sound in principle, and that *the standard result $\gamma_\varphi^{AAK}(T)$ can be reproduced using GZ's method*, provided that it is applied with slightly more care to correctly account for recoil effects (i.e. the fact that the energy of an electron changes when it absorbs or emits a photon). We believe that this finding conclusively resolves the controversy in favor of AAK and company; hopefully, it will also serve to revive appreciation for the merits of GZ's influence functional approach.

The premise for understanding how $\gamma_\varphi^{\rm AAK}$ can be reproduced with GZ's methods was that we had carried out a painfully detailed analysis and rederivation of GZ's calculation, with the aim of establishing to what extent their method is related to the standard Keldysh diagrammatic approach. As it turned out, the two methods are essentially equivalent, and GZ obtained unconventional results only because a certain "Pauli factor" $(\tilde\delta-2\tilde\rho^0)$ occuring in $\tilde S_R$ was not treated sufficiently carefully, where $\tilde\rho^0$ is the single-particle density matrix. That their treatment of this Pauli factor was dubious had of course been understood and emphasized before: first and foremost it was correctly pointed out in [16] that GZ's treatment of the Pauli factor caused their expression for $\gamma_\varphi^{\rm GZ}$ to aquire an artificial ultraviolet divergence, which then produces the term $\gamma_\varphi^{0,{\rm GZ}}$, whereas no such divergence is present in diagrammatic calculations. GZ's treatment of $(\tilde\delta-2\tilde\rho^0)$ was also criticized, in various related contexts, by several other authors [10, 11, 14, 15, 17]. However, none of these works (including our own [14], which, in retrospect, missed the main point, namely recoil) had attempted to diagnose the nature of the Pauli factor problem *with sufficient precision to allow a successful remedy to be devised within the influence functional framework*.

This will be done in the present paper. Working in the time domain, GZ represent $(\tilde{\delta} - 2\rho^0(t))$ as $1 - 2n_0\big[\tilde{h}_0(t)/2T\big]$, where $n_0$ is the Fermi function and $\tilde{h}_0(t)$ the free part of the electron energy. GZ assumed that $\tilde{h}_0(t)$ does not change during the diffusive motion, because scattering off impurities is elastic. Our diagnosis is that this assumption *unintentionally neglects recoil effects* (as first pointed out in [10]), because the energy of an electron actually does change at each interaction vertex, i.e. each time it emits or absorbs a photon. The remedy (not found in [10]) is to transform from the time to the frequency domain, in which $(\tilde{\delta} - 2\tilde{\rho}^0)$ is represented by $1 - 2n_0[\hbar(\bar{\varepsilon} - \bar{\omega})] = \tanh[\hbar(\bar{\varepsilon} - \bar{\omega})/2T]$, where $\hbar\bar{\omega}$ is the energy change experienced by an electron with energy $\hbar\bar{\varepsilon}$ at an interaction vertex. Remarkably, this simple change of representation from the time to the frequency domain is sufficient to recover $\gamma_\varphi^{\rm AAK}$. Moreover, the ensuing calculation is free of ultraviolet or infrared divergencies, and no cut-offs of any kind have to be introduced by hand.

The present paper has two main aims: firstly, to concisely explain the nature of the Pauli factor problem and its remedy; and secondly, to present a transparent calculation of $\gamma_\varphi$, using only a few lines of simple algebra. (Actually, we shall only present a "rough" version of the calculation here, which reproduces the qualitative behavior of $\gamma_\varphi^{\rm AAK}(T)$; an improved version, which achieves quantitative agreement with AAK's result for the magnetoconductance [with an error of at most 4% for quasi-1-D wires], will be published separately [19]).

We have made an effort to keep the paper reasonably short and to the point, and not to dwell on technical details of interest only to the experts. Regrettably, this has had the consequence that the present paper is not fully self-contained: it builds on an extensive and very detailed analysis that could not and has not been included here. These details have been written up in the form of five lengthy appendices. Although the present paper is written such that, once one accepts its starting point [Eqs. (8.1) to Eq. (8.4)], the rest of the discussion can easily be followed step by step, readers interested in an honest derivation of the starting point will have to consult the appendices. For those readers (presumably the majority) with no time or inclination to read lengthy appendices, a concise appendix at the end of this paper summarizes (without derivations) the main steps and approximations involved in obtaining the influence functional. We shall publish the five long appendices B to F separately [20], in the belief that *all* relevant details should be publicly accessible when dealing with a controversy, for the benefit of those willing to "read the fine print". Below we shall refer to these appendices as though they were a part of the present paper, and briefly summarize their contents here:

In App. B, we rederive the influence functional and effective action of GZ, following their general strategy in spirit, but introducing some improvements. The most important differences are: (i) instead of using the coordinate-momentum path integral $\int\mathcal{D}(\boldsymbol{RP})$ of GZ, we use a "coordinates-only" version $\int\tilde{\mathcal{D}}'\boldsymbol{R}$,

since this enables the Pauli factor to be treated more accurately; and (ii), we are careful to perform thermal weigthing at an initial time $t_0 \to -\infty$ (which GZ do not do), which is essential for obtaining properly energy-averaged expressions and for reproducing perturbative results: the standard diagrammatic Keldysh perturbation expansion for the Cooperon in powers of the interaction propagator is generated if, *before disorder averaging*, the influence functional is expanded in powers of $(i\tilde{S}_R + \tilde{S}_I)$. In App. C we review how a general path integral expression derived for the conductivity in App. B can be rewritten in terms of the familiar Cooperon propagator, and thereby related to the standard relations familiar from diagrammatic perturbation theory. In particular, we review the Fourier transforms required to get a path integral $\tilde{P}^\varepsilon$ properly depending on the energy variable $\hbar\varepsilon$ relevant for thermal weighting. Appendix D gives an explicit time-slicing definition of the "coordinates-only" path integral $\int \tilde{\mathcal{D}}' \boldsymbol{R}$ used in App. B. Finally, for reference purposes, we collect in Apps. E and F some standard material on the diagrammatic technique (although this is bread-and-butter knowledge for experts in diagrammatic methods and available elsewere, it is useful to have it summarized here in a notation consistent with the rest of our analysis). App. E summarizes the standard Keldysh approach in a way that emphasizes the analogy to our influence functional approach, and App. F collects some standard and well-known results used for diagrammatic disorder averaging. Disorder averaging is discussed last for a good reason: one of the appealing features of the influence functional approach is that most of the analysis can be performed *before* disorder averaging, which, if at all, only has to be performed at the very end.

## 2. Main results of influence functional approach

We begin by summarizing the main result of GZ's influence functional approach. Our notations and also the content of of our some formulas are not identical to those of GZ, and in fact differ from their's in important respects. Nevertheless, we shall refer to them as "GZ's results", since we have (re)derived them (see App. B [20] for details) in the spirit of GZ's approach.

The Kubo formula represents the DC conductivity $\sigma_{\rm DC}$ in terms of a retarded current-current correlator $\langle[\hat{\boldsymbol{j}}(1), \hat{\boldsymbol{j}}(2)]\rangle$. This correlator can (within various approximations discussed in App. B.5.6, B.5.7 and App. B.6.3) be expressed as follows in terms of a path integral $\tilde{P}^\varepsilon$ representing the propagation of a pair

of electrons with average energy $\hbar\varepsilon$, thermally averaged over energies:

$$\begin{aligned}\sigma_{\rm DC} &= \frac{2}{d}\int dx_2\, \boldsymbol{j}_{11'}\cdot\boldsymbol{j}_{22'}\int(d\varepsilon)[-n'(\hbar\varepsilon)]\int_0^\infty d\tau\, \tilde{P}^{12',\varepsilon}_{21',\rm eff}(\tau)\ ,\\ \tilde{P}^{12',\varepsilon}_{21',\rm eff}(\tau) &= \oint\!\!\!\!\!\!\int_{\boldsymbol{R}^F(-\frac{\tau}{2})=\boldsymbol{r}_{2'}}^{\boldsymbol{R}^F(\frac{\tau}{2})=\boldsymbol{r}_1}\ \oint\!\!\!\!\!\!\int_{\boldsymbol{R}^B(-\frac{\tau}{2})=\boldsymbol{r}_2}^{\boldsymbol{R}^B(\frac{\tau}{2})=\boldsymbol{r}_{1'}}\widetilde{\mathcal{D}}'(\boldsymbol{R})\ e^{\frac{1}{\hbar}[i(\tilde{S}_0^F-\tilde{S}_0^B)-(i\tilde{S}_R+\tilde{S}_I)](\tau)}.\end{aligned} \tag{8.1}$$

The propagator $\tilde{P}^{12',\varepsilon}_{21',\rm eff}(\tau)$, defined for a given impurity configuration, is written in terms of a forward and backward path integral $\oint\!\!\!\!\!\!\int\widetilde{\mathcal{D}}'(\boldsymbol{R})$ between the specified initial and final coordinates and times, which gives the amplitude for an electron with energy $\hbar\varepsilon$ to propagate from $\boldsymbol{r}_{2'}$ at time $-\frac{1}{2}\tau$ to $\boldsymbol{r}_1$ at $\frac{1}{2}\tau$, times the amplitude for it to propagate from $\boldsymbol{r}_{1'}$ at time $\frac{1}{2}\tau$ to $\boldsymbol{r}_2$ at $-\frac{1}{2}\tau$. We shall call these the forward and backward paths, respectively, using an index $a = F, B$ to distinghuish them. $\tilde{S}_0^a = \tilde{S}_0^{F/B}$ are the corresponding free actions, which determine which paths will dominate the path integral. The weak localization correction to the conductivity, $\sigma_{\rm DC}^{\rm WL}$, arises from the "Cooperon" contributions to $\sigma_{\rm DC}$ for which the coordinates $\boldsymbol{r}_1$, $\boldsymbol{r}_1'$, $\boldsymbol{r}_2$ and $\boldsymbol{r}_2'$ all lie close together, and which feature self-returning random walks through the disordered potential landscape for pairs of paths $\boldsymbol{R}^{F/B}$, with path $B$ being the time-reversed version of path $F$, i.e. $\boldsymbol{R}^F(t_3) = \boldsymbol{R}^B(-t_3)$ for $t_3 \in (-\frac{1}{2}\tau, \frac{1}{2}\tau)$. The effect of the other electrons on this propagation is encoded in the influence functional $e^{-(i\tilde{S}_R+\tilde{S}_I)}$ occuring in Eq. (8.1). The effective action $i\tilde{S}_R + \tilde{S}_I$ turns out to have the form [for a more explicit version, see Eq. (8.A.7) in the appendix]:

$$\left\{\begin{array}{c} i\tilde{S}_R(\tau)\\ \tilde{S}_I(\tau)\end{array}\right\} = -\tfrac{1}{2}i\sum_{a,a'=F,B} s_a\int_{-\frac{\tau}{2}}^{\frac{\tau}{2}} dt_{3_a}\int_{-\frac{\tau}{2}}^{t_{3_a}} dt_{4_{a'}}\left\{\begin{array}{c}\tilde{\mathcal{L}}^{a'}_{3_a4_{a'}}\\ s_{a'}\tilde{\mathcal{L}}^{K}_{3_a4_{a'}}\end{array}\right\}. \tag{8.2}$$

Here $s_a$ stands for $s_{F/B} = \pm 1$, and the shorthand $\tilde{\mathcal{L}}_{3_a4'_a} = \tilde{\mathcal{L}}\big[t_{3_a}-t_{4_{a'}}, \boldsymbol{R}^a(t_{3_a})-\boldsymbol{R}^{a'}(t_{4_{a'}})\big]$ describes, in the coordinate-time representation, an interaction propagator linking two vertices on contours $a$ and $a'$. It will be convenient below to Fourier transform to the momentum-freqency representation, where the propagators $\tilde{\mathcal{L}}^K$ and $\tilde{\mathcal{L}}^{a'}$ can be represented as follows [$(d\bar{\omega})(d\bar{\boldsymbol{q}}) \equiv (d\bar{\omega}\, d\bar{\boldsymbol{q}})/(2\pi)^4$]:

$$\tilde{\mathcal{L}}^K_{3_a4_{a'}} \equiv \int(d\bar{\omega})(d\bar{\boldsymbol{q}})e^{i\left(\bar{\boldsymbol{q}}\cdot\left[\boldsymbol{R}^a(t_{3_a})-\boldsymbol{R}^{a'}(t_{4_{a'}})\right]-\bar{\omega}(t_{3_a}-t_{4_{a'}})\right)}\tilde{\mathcal{L}}^K_{\bar{\boldsymbol{q}}}(\bar{\omega})\,, \tag{8.3a}$$

$$\tilde{\mathcal{L}}^{a'}_{3_a4_{a'}} \equiv \left\{\begin{array}{ll}\big[(\tilde{\delta}-2\tilde{\rho}^0)\tilde{\mathcal{L}}^R\big]_{3_a4_F} & \text{if}\quad a'=F\,,\\ \big[\tilde{\mathcal{L}}^A(\tilde{\delta}-2\tilde{\rho}^0)\big]_{4_B3_a} & \text{if}\quad a'=B\,,\end{array}\right. \tag{8.3b}$$

$$\equiv \int(d\bar{\omega})(d\bar{\boldsymbol{q}})e^{is_{a'}\left(\bar{\boldsymbol{q}}\cdot\left[\boldsymbol{R}^a(t_{3_a})-\boldsymbol{R}^{a'}(t_{4_{a'}})\right]-\bar{\omega}(t_{3_a}-t_{4_{a'}})\right)}\tilde{\mathcal{L}}^{a'}_{\bar{\boldsymbol{q}}}(\bar{\omega})\,. \tag{8.3c}$$

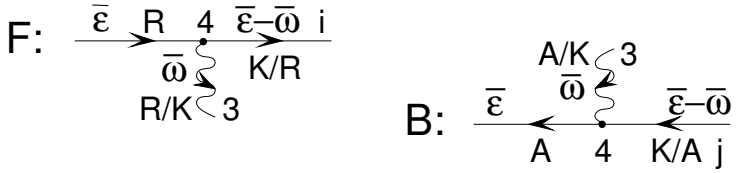


*Figure 8.1.* Structure of vertices on the forward or backward contours of Keldysh perturbation theory. F: the combinations $\tilde{G}^K_{i_F 4_F}\tilde{\mathcal{L}}^R_{34_F}$ and $\tilde{G}^R_{i_F 4_F}\tilde{\mathcal{L}}^K_{34_F}$ occur if vertex 4 lies on the upper forward contour. B: the combinations $\tilde{\mathcal{L}}^A_{4_B 3}\tilde{G}^K_{4_B j_B}$ and $\tilde{\mathcal{L}}^K_{4_B 3}\tilde{G}^A_{4_B j_B}$ occur if vertex 4 lies on the lower contour. Arrows point from the second to first indices of propagators.

[Note the sign $s_{a'}$ in the Fourier exponential in Eq. (8.3c); it reflects the opposite order of indices in Eq. (8.3b), namely 34 for $F$ vs. 43 for $B$.] Here $\tilde{\mathcal{L}}^K$ is the Keldysh interaction propagator, while $\tilde{\mathcal{L}}^{F/B}$, to be used when time $t_{4_{a'}}$ lies on the forward or backward contours, respectively, represent "effective" retarded or advanced propagators, modified by a "Pauli factor" $(\tilde{\delta} - 2\tilde{\rho}^0)$ (involving a Dirac-delta $\tilde{\delta}_{ij}$ and single-particle density matrix $\tilde{\rho}^0_{ij}$ in coordinate space), the precise meaning of which will be discussed below. $\tilde{\mathcal{L}}^{K,R,A}_{\bar{\boldsymbol{q}}}(\bar{\omega})$ denote the Fourier transforms of the standard Keldysh, retarded, or advanced interaction propatators. For the screened Coulomb interaction in the unitary limit, they are given by

$$\overline{\mathcal{L}}^R_{\bar{\boldsymbol{q}}}(\bar{\omega}) = [\overline{\mathcal{L}}^A_{\bar{\boldsymbol{q}}}(\bar{\omega})]^* = -\frac{E^0_{\bar{\boldsymbol{q}}} - i\bar{\omega}}{2\nu E^0_{\bar{\boldsymbol{q}}}} = -\frac{[\overline{\mathcal{D}}^0_{\bar{\boldsymbol{q}}}(\bar{\omega})]^{-1}}{2\nu E^0_{\bar{\boldsymbol{q}}}} \,, \tag{8.4a}$$

$$\overline{\mathcal{L}}^K_{\bar{\boldsymbol{q}}}(\bar{\omega}) = 2\,i\coth(\hbar\bar{\omega}/2T)\,\mathrm{Im}[\overline{\mathcal{L}}^R_{\bar{\boldsymbol{q}}}(\bar{\omega})] \,, \tag{8.4b}$$

$$\overline{\mathcal{C}}^0_{\bar{\boldsymbol{q}}}(\bar{\omega}) = \frac{1}{E_{\bar{\boldsymbol{q}}} - i\bar{\omega}} \,, \qquad \overline{\mathcal{D}}^0_{\bar{\boldsymbol{q}}}(\bar{\omega}) = \frac{1}{E^0_{\bar{\boldsymbol{q}}} - i\bar{\omega}} \,, \tag{8.4c}$$

$$E^0_{\bar{\boldsymbol{q}}} = D\bar{\boldsymbol{q}}^2 \,, \qquad E_{\bar{\boldsymbol{q}}} = D\bar{\boldsymbol{q}}^2 + \gamma_H \,, \tag{8.4d}$$

where, for later reference, we have also listed the Fourer transforms of the bare diffuson $\overline{\mathcal{D}}^0$ and Cooperon $\overline{\mathcal{C}}^0$ (where $\gamma_H$ is the dephasing rate of the latter in the presence of a magnetic field, $D$ the diffusion constant and $\nu$ the density of states per spin). Finally, $\tilde{\mathcal{L}}^{a'}_{\bar{\boldsymbol{q}}}(\bar{\omega})$ in Eq. (8.3c) is defined as

$$\tilde{\mathcal{L}}^{F/B}_{\bar{\boldsymbol{q}}}(\bar{\omega}) = \tanh[\hbar(\varepsilon - \bar{\omega})/2T]\,\tilde{\mathcal{L}}^{R/A}_{\bar{\boldsymbol{q}}}(\bar{\omega}) \,, \tag{8.4e}$$

where $\hbar\varepsilon$ is the same energy as that occuring in the thermal weighting factor $[-n'(\hbar\varepsilon)]$ in the first line of Eq. (8.1).

Via the influence functional, the effective action (8.2) concisely incorporates the effects of interactions into the path integral approach. $\tilde{S}_I$ describes the *classical* part of the effective environment, and if one would replace the factor

$\coth(\hbar\bar{\omega}/2T)$ in $\tilde{\mathcal{L}}^K_{\vec{q}}(\bar{\omega})$ by $2T/\hbar\bar{\omega}$ (as is possible for high temperatures) it corresponds to the contribution calculated by AAK [9]. With $\tilde{S}_R$, GZ succeeded to additionally also include the quantum part of the environment, and in particular, via the Pauli factor $(\tilde{\delta} - 2\tilde{\rho}^0)$, to properly account for the Pauli principle.

Casual readers are asked to simply accept the above equations as starting point for the remainder of this paper, and perhaps glance through App. A to get an idea of the main steps and approximations involved. Those interested in a detailed derivation are referred to App. B (where $\tilde{S}_{R/I}$ are obtained in Sec. B.5.8). It is also shown there [Sec. B.6] that the standard results of diagrammatic Keldysh perturbation theory can readily be reproduced from the above formalism by expanding the influence functional $e^{-(i\tilde{S}_R+\tilde{S}_I)/\hbar}$ in powers of $(i\tilde{S}_R+\tilde{S}_I)/\hbar$. For present purposes, simply note that such an equivalence is entirely plausible in light of the fact that our effective action (8.2) is linear in the effective interaction propagators $\tilde{\mathcal{L}}$, a structure typical for generating functionals for Feynman diagrams.

## 3. Origin of the Pauli factor

The occurence of the Pauli factor $(\tilde{\delta} - 2\tilde{\rho}^0)$ in $\tilde{S}_R$ was first found by GZ in precisely the form displayed in the position-time representation of the effective action used in Eq. (8.2). However, their subsequent treatment of this factor differs from ours, in a way that will be described below. In particular, they did not represent this factor in the frequency representation, as in our Eq. (8.4e), and this is the most important difference between our analysis and theirs.

The origin of the Pauli factor in the form given by our Eq. (8.4e) can easily be understood if one is familiar with the structure of Keldysh perturbation theory. [For a detailed discussion, see Sec. B.6.2.] First recall two exact relations for the noninteraction Keldysh electron propagator: in the coordinate-time representation, it contains a Pauli factor,

$$\tilde{G}^K_{ij} = \int dx_k \, (\tilde{G}^R - \tilde{G}^A)_{ik}(\tilde{\delta} - 2\tilde{\rho}^0)]_{kj} = \int dx_k \, (\tilde{\delta} - 2\tilde{\rho}^0)_{ik}(\tilde{G}^R - \tilde{G}^A)_{kj} \tag{8.5a}$$

which turns into a $\tanh$ in the coordinate frequency representation:

$$\tilde{G}^K_{ij}(\bar{\omega}) = \tanh(\hbar\bar{\omega}/2T)\Big[\tilde{G}^R_{ij}(\bar{\omega}) - \tilde{G}^A_{ij}(\bar{\omega})\Big] \, . \tag{8.5b}$$

Now, in the Keldysh approach retarded or advanced interaction propagators always occur [see Fig.8.1] together with Keldysh electron propagators, in the combinations $\tilde{G}^K_{i_F 4_F}\tilde{\mathcal{L}}^R_{34_F}$ or $\tilde{\mathcal{L}}^A_{4_B 3}\tilde{G}^K_{4_B j_B}$ where the indices denote coordinates and times. [Likewise, the Keldysh interaction propagators always come in the combinations $\tilde{G}^R_{i_F 4_F}\tilde{\mathcal{L}}^K_{34_F}$ or $\tilde{\mathcal{L}}^K_{4_B 3}\tilde{G}^A_{4_B j_B}$.] In the momentum-frequency representation, the combinations involving $\tilde{G}^K$ therefore turn into $\tilde{\mathcal{L}}^{R/A}_{\vec{q}}(\bar{\omega})\big[\tilde{G}^R -$

$\tilde{G}^A\big]_{\boldsymbol{q}-\bar{\boldsymbol{q}}}(\bar{\varepsilon}-\bar{\omega})\,\tanh[\hbar(\bar{\varepsilon}-\bar{\omega})/2T]$. Thus, *in the frequency representation the Pauli factor is represented as* $\tanh[\hbar(\bar{\varepsilon}-\bar{\omega})/2T]$. Here the variable $\hbar\bar{\varepsilon}$ represents the energy of the electron line on the upper (or lower) Keldysh contour before it enters (or after it leaves) an interaction vertex at which its energy decreases (or increases) by $\hbar\bar{\omega}$ [see Fig. 8.1]. The subtraction of $\bar{\omega}$ in the argument of $\tanh$ thus reflects the physics of recoil: emitting or absorbing a photon causes the electron energy to change by $\hbar\bar{\omega}$, and it is this changed energy $\hbar(\bar{\varepsilon}-\bar{\omega})$ that enters the Fermi functions for the relevant final or initial states.

Of course, in Keldysh perturbation theory, $\hbar\bar{\varepsilon}$ will have different values from one vertex to the next, reflecting the history of energy changes of an electron line as it proceeds through a Feynman diagram. It is possible to neglect this complication in the influence functional approach, if one so chooses, by always using one and the same energy in Eq. (8.4e), which then should be chosen to be the same as that occuring in the thermal weighting factor $[-n'(\hbar\varepsilon)]$, i.e. $\hbar\bar{\varepsilon} = \hbar\varepsilon$. This approximation, which we shall henceforth adopt, is expected to work well if the relevant physics is dominated by low frequencies, at which energy transfers between the two contours are sufficiently small [$\hbar(\bar{\varepsilon}-\varepsilon) \ll T$, so that the electron "sees" essentially the same Fermi function throughout its motion].

Though the origin and neccessity of the Pauli factor is eminently clear when seen in conjunction with Keldysh perturbation theory, it is a rather nontrivial matter to derive it cleanly in the functional integral approach [indeed, this is the main reason for the length of our appendices!]. The fact that GZ got it completely right in the position-time representation of Eq. (8.2) is, in our opinion, a significant and important achievement; unfortunately, however, it did not occur to them to use the frequency representation (8.4e).

## 4. Calculating $\tau_\varphi$ à la GZ

To calculate the decoherence rate $\gamma_\varphi = 1/\tau_\varphi$, one has to find the long-time decay of the Cooperon contribution to the propagator $\tilde{P}^{\varepsilon}_{\text{eff}}(\tau)$ of Eq. (8.1). To do this, GZ proceeded as follows: using a saddle-point approximation for the path integral for the Cooperon, they replaced the sum over all pairs of self-returning paths $\boldsymbol{R}^{F/B}(t_{3_{F/B}})$ by just the contribution $\langle e^{-\frac{1}{\hbar}(i\tilde{S}_R+\tilde{S}_I)(\tau)}\rangle_{\text{rw}}$ of the classical "random walk" paths $\boldsymbol{R}_{\text{rw}}(t)$ picked out by the classical actions $\tilde{S}^a_0$, namely $\boldsymbol{R}^F(t_{3_F}) = \boldsymbol{R}_{\text{rw}}(t_{3_F})$ and $\boldsymbol{R}^B(t_{3_B}) = \boldsymbol{R}_{\text{rw}}(-t_{3_B})$, for which the paths on the forward and backward Keldysh contours are *time-reversed* partners. The subscript "rw" indicates that each such classical path is a self-returning random walk through the given disorder potential landscape, and $\langle\ \rangle_{\text{rw}}$ means averaging over all such paths. Next, in the spirit of [21], they replace the average of the exponent over all time-reversed pairs of self-returning random walks, by the exponent of the average, $e^{-F(\tau)}$, where $F(\tau) = \langle i\tilde{S}_R + \tilde{S}_I\rangle_{\text{rw}}$ (cf. Eq. (67)

of [2]). This amounts to expanding the exponent to first order, then averaging, and then reexponentiating. The function $F(\tau)$ thus defined increases with time, starting from $F(0) = 0$, and the decoherence time $\tau_\varphi$ can be defined as the time at which it becomes of order one, i.e. $F(\tau_\varphi) \approx 1$.

To evaluate $\langle i\tilde{S}_R + \tilde{S}_I\rangle_{\rm rw}$, GZ Fourier transform the functions $\tilde{\mathcal{L}}_{3_a 4'_a} = \tilde{\mathcal{L}}[t_{34}, \boldsymbol{R}^a(t_3) - \boldsymbol{R}^{a'}(t_4)]$ occuring in $\tilde{S}_{R/I}$, and average the Fourier exponents using [21] the distribution function for diffusive motion, which gives probability that a random walk that passes point $\boldsymbol{R}_{\rm rw}(t_4)$ at time $t_4$ will pass point $\boldsymbol{R}_{\rm rw}(t_3)$ at time $t_3$, i.e. that it covers a distance $\boldsymbol{R} = \boldsymbol{R}_{\rm rw}(t_3) - \boldsymbol{R}_{\rm rw}(t_4)$ in time $|t_{34}|$:

$$\begin{aligned}\left\langle e^{i\bar{\boldsymbol{q}}\cdot[\boldsymbol{R}_{\rm rw}(t_3)-\boldsymbol{R}_{\rm rw}(t_4)]}\right\rangle_{\rm rw} &\simeq \int d^{\bar{d}}\boldsymbol{R}\left(\frac{\pi}{D|t_{34}|}\right)^{\bar{d}/2} e^{-\boldsymbol{R}^2/(4D|t_{34}|)}\, e^{i\bar{\boldsymbol{q}}\cdot\boldsymbol{R}} \\ &= e^{-\bar{\boldsymbol{q}}^2 D|t_{34}|} \to \tilde{C}^0_{\bar{\boldsymbol{q}}}(|t_{34}|) = e^{-E_{\bar{\boldsymbol{q}}}|t_{34}|}\ . \end{aligned} \tag{8.6}$$

(Here $t_{34} = t_3 - t_4$.) The arrow in the second line makes explicit that if we also account for the fact that such time-reversed pairs of paths are dephased by a magnetic field, by adding a factor $e^{-\gamma_H|t_{34}|}$, the result is simply equal to the bare Cooperon in the momentum-time representation.

Actually, the above way of averaging is somewhat inaccurate, as was pointed out to us by Florian Marquardt: it neglects the fact that the diffusive trajectories between $t_3$ and $t_4$ are part of a larger, *self-returning* trajectory, starting and ending at $\boldsymbol{r}_1 \simeq \boldsymbol{r}_2$ at times $\mp\frac{1}{2}\tau$. It is actually not difficult to include this fact [19], and this turns out to quantitatively improve the numerical prefactor for $\tau_\varphi$ (e.g. in Eq. (8.18) below). However, for the sake of simplicity, we shall here be content with using Eq. (8.6), as GZ did.

Finally, GZ also assumed that the Pauli factor $(\tilde{\delta} - 2\tilde{\rho}^0)$ in $\tilde{S}_R$ remains unchanged throughout the diffusive motion: they use a coordinate-momentum path integral $\int \mathcal{D}\boldsymbol{R}\int\mathcal{D}\boldsymbol{P}$ [instead of our coordinates-only version $\int\widetilde{\mathcal{D}}'\boldsymbol{R}$], in which $(\tilde{\delta} - 2\tilde{\rho}^0)$ is replaced by $[1 - 2n_0(\tilde{h}_0)] = \tanh(\tilde{h}_0/2T)$, and the free-electron energy $\tilde{h}_0(\boldsymbol{R}(t_a), \boldsymbol{P}(t_a)$ is argued to be unchanged throughout the diffusive motion, since impurity scattering is elastic [cf. p. 9205 of [2]: "$n$ depends only on the energy and not on time because the energy is conserved along the classical path"]. Indeed, this is true *between* the two interaction events at times $t_3$ and $t_4$, so that the averaging of Eq. (8.6) *is* permissible. However, as emphasized above, the full trajectory stretches from $-\frac{1}{2}\tau$ to $t_4$ to $t_3$ to $\frac{1}{2}\tau$, and the electron energy *does* change, by $\pm\hbar\bar{\omega}$, at the interaction vertices at $t_4$ and $t_3$. Thus, *GZ's assumption of a time-independent Pauli factor neglects recoil effects*. As argued in the previous section, these can straightforwardly taken into account using Eq. (8.4e), which we shall use below. In contrast, GZ's assumption of time-independent $n$ amounts dropping the $-\hbar\bar{\omega}$ in our $\tanh[\hbar(\varepsilon - \bar{\omega})/2T]$ function.

If one uses GZ's assumptions to average Eq. (8.2), but uses the proper $\tanh[\hbar(\varepsilon-\bar\omega)/2T]$ function, one readily arrives at

$$\left\{\begin{array}{c}\langle i\tilde S_R\rangle_{\rm rw}\\ \langle\tilde S_I\rangle_{\rm rw}\end{array}\right\}=2{\rm Re}\left[-\tfrac{1}{2}i\int(d\bar\omega)(d\bar{\boldsymbol q})\left\{\begin{array}{c}\overline{\mathcal L}^F_{\bar{\boldsymbol q}}(\bar\omega)\\ \overline{\mathcal L}^K_{\bar{\boldsymbol q}}(\bar\omega)\end{array}\right\}\Big[f^{\rm self}-f^{\rm vert}\Big](\tau)\right], \quad (8.7)$$

where $f^{\rm self}-f^{\rm vert}$ are the first and second terms of the double time integral

$$\int_{-\frac{\tau}{2}}^{\frac{\tau}{2}}dt_3\int_{-\frac{\tau}{2}}^{t_3}dt_4\,e^{-i\bar\omega t_{34}}\Big\langle e^{i\boldsymbol q\cdot[\boldsymbol R_{\rm rw}(t_3)-\boldsymbol R_{\rm rw}(t_4)]}-e^{i\boldsymbol q\cdot[\boldsymbol R_{\rm rw}(-t_3)-\boldsymbol R_{\rm rw}(t_4)]}\Big\rangle_{\rm rw}, \quad (8.8)$$

corresponding to self-energy ($a=a'=F$) and vertex ($a\neq a'=F$) contributions, and the $2\,{\rm Re}[\ ]$ in Eq. (8.7) comes from adding the contributions of $a'=F$ and $B$. Performing the integrals in Eq. (8.8), we find

$$f^{\rm self}(\tau) \;=\; \overline{\mathcal C}^0_{\bar{\boldsymbol q}}(-\bar\omega)\tau \;+\; \big[\overline{\mathcal C}^0_{\bar{\boldsymbol q}}(-\bar\omega)\big]^2\left[e^{-\tau(E_{\bar{\boldsymbol q}}+i\bar\omega)}-1\right], \quad (8.9a)$$

$$f^{\rm vert}(\tau) \;=\; \overline{\mathcal C}^0_{\bar{\boldsymbol q}}(\bar\omega)\left[\frac{e^{-i\bar\omega\tau}-1}{-i\bar\omega}+\frac{e^{-E_{\bar{\boldsymbol q}}\tau}-1}{E_{\bar{\boldsymbol q}}}\right]. \quad (8.9b)$$

Of all terms in Eqs. (8.9), the first term of $f^{\rm self}$, which is linear in $\tau$, clearly grows most rapidly, and hence dominates the leading long-time behavior. Denoting the associated contribution to Eq. (8.7) by $\frac{1}{\hbar}\langle i\tilde S_R/\tilde S_I\rangle_{\rm rw}^{\rm leading,self}\equiv\tau\gamma_\varphi^{R/I,{\rm self}}$, the corresponding rates $\gamma_\varphi^{R/I,{\rm self}}$ obtained from Eqs. (8.7) and (8.9) are:

$$\gamma_\varphi^{R,{\rm self}} \;=\; \int(d\bar\omega)(d\bar{\boldsymbol q})\tanh\left[\frac{\hbar(\varepsilon-\bar\omega)}{2T}\right]\;2{\rm Re}\left[\frac{\frac{1}{2}i(E^0_{\bar{\boldsymbol q}}-i\bar\omega)}{2\nu E^0_{\bar{\boldsymbol q}}(E_{\bar{\boldsymbol q}}+i\bar\omega)}\right], \quad (8.10a)$$

$$\gamma_\varphi^{I,{\rm self}} \;=\; \int(d\bar\omega)(d\bar{\boldsymbol q})\coth\left[\frac{\hbar\bar\omega}{2T}\right]\;2{\rm Re}\left[\frac{\bar\omega}{2\nu E^0_{\bar{\boldsymbol q}}(E_{\bar{\boldsymbol q}}+i\bar\omega)}\right]. \quad (8.10b)$$

Let us compare these results to those of GZ, henceforth using $\gamma_H=0$. Firstly, both our $\gamma_\varphi^{I,{\rm self}}$ and $\gamma_\varphi^{R,{\rm self}}$ are nonzero. In contrast, in their analysis GZ concluded that $\langle\tilde S_R\rangle_{\rm rw}=0$. The reason for the latter result is, evidently, their neglect of recoil effects: indeed, if we drop the $-\hbar\bar\omega$ from the $\tanh$-factor of Eq. (8.10a), we would find $\gamma_\varphi^R=0$ and thereby recover GZ's result, since the real part of the factor in square brackets is odd in $\bar\omega$.

Secondly and as expected, we note that Eq. (8.10b) for $\gamma_\varphi^{I,{\rm self}}$ agrees with that of GZ, as given by their equation (71) of [2] for $1/\tau_\varphi$, i.e. $\gamma_\varphi^{I,{\rm self}}=\gamma_\varphi^{\rm GZ}$. [To see the equivalence explicitly, use Eq. (8.A.9).] Noting that the $\int d\bar\omega$-integral in Eq. (8.10b) evidently diverges for large $\bar\omega$, GZ cut off this divergence at $1/\tau_{\rm el}$ (arguing that the diffusive approximation only holds for time-scales longer than

$\tau_{\rm el}$, the elastic scattering time). For example, for quasi-1-dimensional wires, for which $\int (d\bar{\boldsymbol{q}}) = a^{-2}\int dq/(2\pi)$ can be used ($a^2$ being the cross section, so that $\sigma_1 = a^2\sigma_{\rm DC}^{\rm Drude}$ is the conductivity per unit length, with $\sigma_{\rm DC}^{\rm Drude} = 2e^2\nu D$), they obtain (cf. (76) of [2]):

$$\frac{1}{\tau_\varphi^{\rm GZ}} \simeq \frac{e^2\sqrt{2D}}{\sigma_1}\int_{\frac{1}{\tau_\varphi^{\rm GZ}}}^{\frac{1}{\tau_{\rm el}}} (d\bar{\omega})\coth\left[\frac{\hbar\bar{\omega}}{2T}\right] \simeq \frac{e^2}{\pi\sigma_1}\sqrt{\frac{2D}{\tau_{\rm el}}}\left[\frac{2T\sqrt{\tau_{\rm el}\tau_\varphi^{\rm GZ}}}{\hbar}+1\right], \tag{8.11}$$

[The use of a self-consistently-determined lower cut-off is explained in Sec.6]. Thus, they obtained a temperature-independent contribution $\gamma_\varphi^{0,\rm GZ}$ from the +1 term, which is the result that ingited the controversy.

However, we thirdly observe that, due to the special form of the retarded interaction propagator in the unitary limit, the real parts of the last factors in square brackets of Eqs. (8.10a) and (8.10b) are actually *equal* (for $\gamma_H = 0$). Thus, the ultraviolet divergence of $\gamma_\varphi^{I,\rm self}$ is *cancelled* by a similar divergence of $\gamma_\varphi^{R,\rm self}$. Consequently, the total decoherence rate coming from self-energy terms, $\gamma_\varphi^{\rm self} = \gamma_\varphi^{I,\rm self} + \gamma_\varphi^{R,\rm self}$, is free of ultraviolet divergencies. Thus we conclude that the contribution $\gamma_\varphi^{0,\rm GZ}$ found by GZ is an artefact of their neglect of recoil, as is their claimed "decoherence at zero temperature".

## 5. Dyson Equation and Cooperon self energy

The above results for $\gamma_\varphi^{R,\rm self} + \gamma_\varphi^{I,\rm self}$ turn out to agree completely with those of a standard calculation of the Cooperon self energy $\tilde{\Sigma}$ using diagrammatic impurity averaging [details of which are summarized in Appendix F]. We shall now summarize how this comes about.

Calculating $\tilde{\Sigma}$ is an elementary excercise within diagrammatic perturbation theory, first performed in [22]. However, to facilitate comparison with the influence functional results derived above, we proceed differently: We have derived [Sec. B.6.1] a general expression [23], before impurity averaging, for the Cooperon self-energy of the form $\tilde{\Sigma} = \sum_{aa'}\left[\tilde{\Sigma}^I_{aa'} + \tilde{\Sigma}^R_{aa'}\right]$, which keeps track of which terms originate from $i\tilde{S}_R$ or $\tilde{S}_I$, and which contours $a, a' = F/B$ the vertices sit on. This expression agrees, as expected, with that of Keldysh perturbation theory, before disorder averaging; it is given by Eq. (8.A.10) and illustrated by Fig. 8.A.10 in App. A. We then disorder average using standard diagrammatic techniques. For reference purposes, some details of this straightforward excercise are collected in Appendix F.2.

For present purposes, we shall consider only the "self-energy contributions" ($a = a'$) to the Cooperon self energy, and neglect the "vertex contributions" ($a \neq a'$), since above we likewise extracted $\gamma_\varphi^{R/I}$ from the self-

energy contributions to the effective action, $\langle \tilde{S}_{R/I} \rangle_{\rm rw}^{\rm leading,self}$. After impurity averaging, the Cooperon then satisfies a Dyson equation of standard form, $\overline{\mathcal{C}}_{\boldsymbol{q}}^{\rm self}(\omega) = \overline{\mathcal{C}}_{\boldsymbol{q}}^{0}(\omega) + \overline{\mathcal{C}}_{\boldsymbol{q}}^{0}(\omega)\, \overline{\Sigma}_{\boldsymbol{q}}^{\rm self}(\omega)\, \overline{\mathcal{C}}_{\boldsymbol{q}}^{\rm self}(\omega)$, with standard solution:

$$\overline{\mathcal{C}}_{\boldsymbol{q}}^{\rm self}(\omega) \;\; = \;\; \frac{1}{E_{\boldsymbol{q}} - i\omega - \overline{\Sigma}_{\boldsymbol{q}}^{\rm self}(\omega)} \; , \tag{8.12}$$

where $\overline{\Sigma}^{R/I,{\rm self}} = \sum_a \overline{\Sigma}_{aa}^{R/I,{\rm self}}$, with $\overline{\Sigma}_{\boldsymbol{q},FF}^{R/I,{\rm self}}(\omega) = \Big[\overline{\Sigma}_{\boldsymbol{q},BB}^{R/I,{\rm self}}(-\omega)\Big]^*$, and

$$\overline{\Sigma}_{\boldsymbol{q},FF}^{I,{\rm self}}(\omega) \;\equiv\; -\frac{1}{\hbar}\int (d\bar{\omega})(d\bar{\boldsymbol{q}})\coth\left[\frac{\hbar\bar{\omega}}{2T}\right] {\rm Im}\big[\overline{\mathcal{L}}_{\bar{\boldsymbol{q}}}^{R}(\bar{\omega})\big]\, \overline{\mathcal{C}}_{\boldsymbol{q}-\bar{\boldsymbol{q}}}^{0}(\omega-\bar{\omega}) \; ,$$

$$\begin{aligned}\overline{\Sigma}_{\boldsymbol{q},FF}^{R,{\rm self}}(\omega) \;\equiv\; \frac{1}{\hbar}\int (d\bar{\omega})(d\bar{\boldsymbol{q}})\Bigg\{ &\tanh\Big[\frac{\hbar(\varepsilon+\frac{1}{2}\omega-\bar{\omega})}{2T}\Big]\, \tfrac{1}{2} i\overline{\mathcal{L}}_{\bar{\boldsymbol{q}}}^{R}(\bar{\omega}) \\ &\times \Big[\overline{\mathcal{C}}_{\boldsymbol{q}-\bar{\boldsymbol{q}}}^{0}(\omega-\bar{\omega}) + \big[\overline{\mathcal{D}}_{\bar{\boldsymbol{q}}}^{0}(\bar{\omega})\big]^2\Big(\big[\overline{\mathcal{C}}_{\boldsymbol{q}}^{0}(\omega)\big]^{-1} + \big[\overline{\mathcal{D}}_{\bar{\boldsymbol{q}}}^{0}(\bar{\omega})\big]^{-1}\Big)\Big]\Bigg\}.\end{aligned} \tag{8.13}$$

In Eq. (8.13), the terms proportional to $\big(\overline{\mathcal{D}}^0\big)^2\big[\big(\overline{\mathcal{C}}^0\big)^{-1} + \big(\overline{\mathcal{D}}^0\big)^{-1}\big]$ stem from the so-called Hikami contributions, for which an electron line changes from $\tilde{G}^{R/A}$ to $\tilde{G}^{A/R}$ to $\tilde{G}^{R/A}$. As correctly emphasized by AAG [16] and AAV [17], such terms are missed by GZ's approach of averaging only over time-reversed pairs of paths, since they stem from paths that are not time-reversed pairs.

Now, the standard way to define a decoherence rate for a Cooperon of the form (8.12) is as the "mass" term that survives in the denominator when $\omega = E_{\boldsymbol{q}} = 0$, i.e. $\gamma_\varphi^{\rm self} = -\overline{\Sigma}_{\boldsymbol{0}}^{\rm self}(0) = -2{\rm Re}\left[\overline{\Sigma}_{FF}^{I+R,{\rm self}}\right]$. In this limit the contribution of the Hikami terms vanishes identically, as is easily seen by using the last of Eqs. (8.4a), and noting that ${\rm Re}[i(\overline{\mathcal{D}}^0)^{-1}(\overline{\mathcal{D}}^0)^2(\overline{\mathcal{D}}^0)^{-1}] = {\rm Re}[i] = 0$. (The realization of this fact came to us as a surprise, since AAG and AAV had argued that GZ's main mistake was their neglect of Hikami terms [16, 17], thereby implying that the contribution of these terms is not zero, but essential.) The remaining (non-Hikami) terms of Eq. (8.13) agree with the result for $\tilde{\Sigma}$ of AAV [17] and reproduce Eqs. (8.10) given above, in other words:

$$\gamma_\varphi^{\rm self} = [-\overline{\Sigma}_{\boldsymbol{0}}^{\rm self}(0)] = \frac{1}{\tau\,\hbar}\langle i\tilde{S}_R + \tilde{S}_I\rangle_{\rm rw}^{\rm leading,self} \; . \tag{8.14}$$

Thus, the Cooperon mass term $-\overline{\Sigma}_{\boldsymbol{0}}^{\rm self}(0)$ agrees identically with the coefficient of $\tau$ in the leading terms of the averaged effective action of the influence functional. This is no coincidence: it simply reflects the fact that averaging in the exponent amounts to reexponentiating the *average of the first order term* of an

expansion of the exponential, while in calculating the self energy one of course *also* averages the first order term of the Dyson equation. It is noteworthy, though, that for the problem at hand, where the unitary limit of the interaction propagator is considered, it suffices to perform this average exclusively over pairs of time-reversed paths — more complicated paths are evidently not needed, in contrast to the expectations voiced by AAG and AAV [16, 17]. The latter expectations do apply, however, if one consideres forms of the interaction propagator $\overline{\mathcal{L}}^R_{\bar{\boldsymbol{q}}}(\bar{\omega})$ more general than the unitary limit of (8.4a) (i.e. not proportional to $\big[\overline{\mathcal{D}}^0_{\bar{\boldsymbol{q}}}(\bar{\omega})\big]^{-1}$). Then, the Hikami contribution to $\gamma_\varphi^{\rm self} = -\overline{\Sigma}^{\rm self}_{\boldsymbol{0}}(0)$ indeed does not vanish; instead, by noting that for $\omega = \boldsymbol{q} = \gamma_H$ the second line of Eq. (8.13) can always be written as $2{\rm Re}\big[\overline{\mathcal{D}}^0_{\bar{\boldsymbol{q}}}(\bar{\omega})\big]$, we obtain

$$\gamma_\varphi^{\rm self} = \frac{1}{\hbar}\int (d\bar{\omega})(d\bar{\boldsymbol{q}})\left\{\coth\Big[\frac{\hbar\bar{\omega}}{2T}\Big] + \tanh\Big[\frac{\hbar(\varepsilon-\bar{\omega})}{2T}\Big]\right\} \times{\rm Im}\big[\overline{\mathcal{L}}^R_{\bar{\boldsymbol{q}}}(\bar{\omega})\big]\,\frac{2E^0_{\bar{\boldsymbol{q}}}}{(E^0_{\bar{\boldsymbol{q}}})^2+\bar{\omega}^2}\;, \tag{8.15}$$

which is the form given by AAV [17].

## 6. Vertex contributions

Eq. (8.10b) for $\gamma_\varphi^{I,{\rm self}}$ has the deficiency that its frequency integral is *infrared* divergent (for $\bar{\omega}\to 0$) for the quasi-1 and 2-dimensional cases, as becomes explicit once its $\boldsymbol{q}$-integral has been performed [as in Eq. (8.11)]. This problem is often dealt with by arguing that small-frequency environmental fluctuations that are slower than the typical time scale of the diffusive trajectories are, from the point of view of the diffusing electron, indistuingishable from a static field and hence cannot contribute to decoherence. Thus, a low-frequency cutoff $\gamma_\varphi$ is inserted by hand into Eqs. (8.10) [i.e. $\int_0 d\bar{\omega}\to\int_{\gamma_\varphi} d\bar{\omega}$], and $\gamma_\varphi$ determined selfconsistently. This procedure was motivated in quite some detail by AAG in Ref. [16], and also adopted by GZ in Ref. [2] [see Eq. (8.11) above]. However, as emphasized by GZ in a subsequent paper [3], it has the serious drawback that it does not necessarily reproduce the correct functional form for the Cooperon in the time domain; e.g., in $\bar{d}=1$ dimensions, the Cooperon is known [9] to decay as $e^{-a(\tau/\tau_\varphi)^{3/2}}$, i.e. with a nontrivial power in the exponent, whereas a "Cooperon mass" would simply give $e^{-\tau/\tau_\varphi}$.

A cheap fix for this problem would be to take the above idea of a self-consistent infrared cutoff one step further, arguing that the Cooperon will decay as $e^{-\tau\gamma_\varphi^{\rm self}(\tau)}$, where $\gamma_\varphi^{\rm self}(\tau)$ is a *time-dependent* decoherence rate, whose time-dependence enters via a time-dependent infrared cutoff. Concretely, using

Eqs. (8.14) and (8.10), one would write

$$\gamma_\varphi^{\rm self}(\tau) \;=\; 2\int_{1/\tau}^{\infty}(d\bar\omega)\,\bar\omega\left\{\coth\left[\frac{\hbar\bar\omega}{2T}\right]+\tfrac{1}{2}\sum_{s=\pm}s\tanh\left[\frac{\hbar(\varepsilon-s\bar\omega)}{2T}\right]\right\} \times\int\frac{(d\bar{\boldsymbol{q}})}{\hbar\nu}\frac{1}{(D\bar{\boldsymbol{q}}^2)^2+\bar\omega^2}\;. \tag{8.16}$$

It is straightforward to check [using steps analogous to those used below to obtain Eq. (8.18)] that in $\bar d = 1$ dimensions, the leading long-time dependence is $\gamma_\varphi^{\rm self}(\tau)\propto\tau^{1/2}$, so that this cheap fix does indeed produce the desired $e^{-a(\tau/\tau_\varphi)^{3/2}}$ behavior.

The merits of this admittedly rather ad hoc cheap fix can be checked by doing a better calculation: It is well-known that the proper way to cure the infrared problems is to include "vertex contributions", having interactions vertices on opposite contours. In fact, the original calculation of AAK [9] in effect did just that. Likewise, although GZ neglected vertex contributions in [2], they subsequently included them in [3], exploiting the fact that in the influence functional approach this is as straightforward as calculating the self-energy terms: one simply has to include the contributions to $\langle i\tilde S_R/\tilde S_I\rangle_{\rm rw}$ of the vertex function $-f^{\rm vert}$ in Eq. (8.7), too. The leading contribution comes from the first term in Eq. (8.9b), to be called $\langle i\tilde S_R/\tilde S_I\rangle_{\rm rw}^{\rm leading,vert}$, which gives a contribution identical to $\langle i\tilde S_R/\tilde S_I\rangle_{\rm rw}^{\rm leading,self}$, but multiplied by an extra factor of $-\frac{\sin(\bar\omega\tau)}{\bar\omega\tau}$ under the integral. Thus, if we collect all contributions to Eq. (8.7) that have been termed "leading", our final result for the averaged effective action is $\frac{1}{\hbar}\langle i\tilde S_R+\tilde S_I\rangle_{\rm rw}^{\rm leading}\equiv F_{\bar d}(\tau)$, with

$$F_{\bar d}(\tau) \;=\; \tau\int(d\bar\omega)\,\bar\omega\left\{\coth\left[\frac{\hbar\bar\omega}{2T}\right]+\tanh\left[\frac{\hbar(\varepsilon-\bar\omega)}{2T}\right]\right\}\left(1-\frac{\sin(\bar\omega\tau)}{\bar\omega\tau}\right) \times\int\frac{(d\bar{\boldsymbol{q}})}{\hbar\nu}\frac{1}{(D\bar{\boldsymbol{q}}^2)^2+\bar\omega^2}\;. \tag{8.17}$$

This is our main result: an expression for the decoherence function $F_{\bar d}(\tau)$ that is both ultraviolet and infrared convergent, due to the $(\coth+\tanh)$ and $(1-\sin)$-combinations, respectively, as will be checked below. Comparing this to Eqs. (8.16), we note that $F_{\bar d}(\tau)$ has precisely the same form as $\tau\gamma_\varphi^{\rm self}(\tau)$, except that the infrared cutoff now occurs in the $\int(d\bar\omega)$ integrals through the $(1-\sin)$ combination. Thus, the result of including vertex contributions fully confirms the validity of using the cheap fix replacement $\int_0(d\bar\omega)\to\int_{1/\tau}(d\bar\omega)$, the only difference being that the cutoff function is smooth instead of sharp (which will somewhat change the numerical prefactor of $\tau_\varphi$).

It turns out to be possible to also obtain Eq. (8.17) [and in addition *all* the "subleading" terms of Eq. (8.7)] by purely diagrammatic means: to this end,

one has to set up and solve a Bethe-Salpeter equation. This is a Dyson-type equation, but with interaction lines transferring energies between the upper and lower contours, so that a more general Cooperon $\overline{\mathcal{C}}^{\varepsilon}_{\boldsymbol{q}}(\Omega_1, \Omega_2)$, with three frequency variables, is needed. Such an analysis will be published elsewhere [19].

To wrap up our rederivation of standard results, let us perform the integrals in Eq. (8.17) for $F_{\bar{d}}(\tau)$ for the quasi-1-dimensional case $\bar{d} = 1$. The $\int (d\bar{\boldsymbol{q}})$-integral yields $\bar{\omega}^{-3/2}\sqrt{D/2}/(\sigma_1\hbar)$. To do the frequency integral, we note that since the $(\coth + \tanh)$-combination constrains the relevant frequencies to be $|\hbar\bar{\omega}| \lesssim T$, the integral is dominated by the small-frequency limit of the integrand, in which $\coth(\hbar\bar{\omega}/2T) \simeq 2T/\hbar\bar{\omega}$, whereas $\tanh$, making a subleading contribution, can be neglected. The frequency integral then readily yields

$$F_1(\tau) \;=\; \frac{4}{3\sqrt{\pi}}\frac{T\tau/\hbar}{g_1(\sqrt{D\tau})} \equiv \frac{4}{3\sqrt{\pi}}\left(\frac{\tau}{\tau_\varphi}\right)^{3/2} , \tag{8.18}$$

so that we correctly obtain the known $e^{-a(\tau/\tau_\varphi)^{3/2}}$ decay for the Cooperon. Here $g_{\bar{d}}(L) = (\hbar/e^2)\sigma_{\bar{d}}L^{\bar{d}-2}$ represents the dimensionless conductance, which is $\gg 1$ for good conductors. The second equality in Eq. (8.18) defines $\tau_\varphi$, where we have exploited the fact that the dependence of $F_1$ on $\tau$ is a simple $\tau^{3/2}$ power law, which we made dimensionless by introducing the decoherence time $\tau_\varphi$. [Following AAG [16], we purposefully arranged numerical prefactors such that none occur in the final Eq. (8.19) for $\tau_\varphi$ below.] Setting $\tau = \tau_\varphi$ in Eq. (8.18) we obtain the self-consistency relation and solution (cf. Eq. (2.38a) of AAG, [16]):

$$\frac{1}{\tau_\varphi} = \frac{T/\hbar}{g_{\bar{d}}(\sqrt{D\tau_\varphi})} , \qquad \Rightarrow \qquad \tau_\varphi = \left(\frac{\hbar^2\sigma_1}{Te^2\sqrt{D}}\right)^{2/3} . \tag{8.19}$$

The second relation is the celebrated result of AAK, which diverges for $T \to 0$. This completes our recalculation of $\gamma_\varphi^{\mathrm{AAK}}$ using GZ's influence functional approach.

Eq. (8.18) can be used to calculate the magnetoconductance for $\bar{d} = 1$ via

$$\sigma_{\mathrm{DC}}^{\mathrm{WL}}(H) = -\frac{\sigma_{\mathrm{DC}}^{\mathrm{Drude}}}{\pi\nu\hbar}\int_0^\infty d\tau\, \tilde{C}^0_{\boldsymbol{r}=0}(\tau)\, e^{-F_1(\tau)} . \tag{8.20}$$

(Here, of course, we have to use $\gamma_H \neq 0$ in $\tilde{C}^0_{\boldsymbol{r}=0}(\tau)$. Comparing the result to AAK's result for the magnetoconductance (featuring an Ai' function for $\bar{d} = 1$), one finds qualitatively correct behavior, but deviations of up to 20% for small magnetic fields $H$. The reason is that our calculation was not sufficiently accurate to obtain the correct numerical prefactor in Eq. (8.18). [GZ did not attempt to calculate it accurately, either]. It turns out [19] that if the averaging

over random walks of Eq. (8.6) is done more accurately, following Marquardt's suggestion of ensuring that the random walks are *self-returning*, the prefactor changes in such a way that the magnetoconductance agrees with that of AAK to within an error of at most 4%. Another improvement that occurs for this more accurate calculation is that the results are well-behaved also for finite $\gamma_H$, which is not the case for our present Eq. (8.10a): for $\gamma_H \neq 0$, the real part of the square brackets contains a term proportional to $\gamma_H/E^0_{\bar{\boldsymbol{q}}}$, which contains an infrared divergence as $\bar{\boldsymbol{q}} \to 0$. This problem disappears if the averaging over paths is performed more accurately [19].

## 7. Discussion and summary

We have shown [in Apps. B to D, as summarized in App. A] that GZ's influence functional approach to interacting fermions is sound in principle, and that standard results from Keldysh diagrammatic perturbation theory can be extracted from it, such as the Feynman rules, the first order terms of a perturbation expansion in the interaction, and the Cooperon self energy.

Having established the equivalence between the two aproaches in general terms, we were able to identify precisely why GZ's treatment of the Pauli factor $(\tilde{\delta} - 2\tilde{\rho}^0)$ occuring $\tilde{S}_R$ was problematic: representing it in the time domain as $\tanh[\tilde{h}_0(t)/2T]$, they assumed it not to change during diffusive motion along time-reversed paths. However, they thereby neglected the physics of recoil, i.e. energy changes of the diffusing electrons by emission or absorption of photons. As a result, GZ's calculation yielded the result $\langle i\tilde{S}^{\rm GZ}_R\rangle_{\rm rw} = 0$. The ultraviolet divergence in $\langle \tilde{S}^{\rm GZ}_I\rangle_{\rm rw}$, which in diagrammatic approaches is cancelled by terms involving a $\tanh$ function, was thus left uncancelled, and instead was cut off at $\bar{\omega} \simeq 1/\tau_{\rm el}$, leading to the conclusion that $\gamma^{\rm GZ}_\varphi(T \to 0)$ is finite.

In this paper, we have shown that the physics of recoil can be included very simply by passing from the time to the frequency representation, in which $(\tilde{\delta} - 2\tilde{\rho}^0)$ is represented by $\tanh[\hbar(\varepsilon - \bar{\omega})/2T]$. Then $\langle i\tilde{S}_R\rangle_{\rm rw}$ is found *not* to equal to zero; instead, it cancels the ultraviolet divergence of $\langle \tilde{S}_I\rangle_{\rm rw}$, so that the total rate $\gamma_\varphi = \gamma^I_\varphi + \gamma^R_\varphi$ reproduces the classical result $\gamma^{\rm AAK}_\varphi$, which goes to zero for $T \to 0$. Interestingly, to obtain this result it was sufficient to average only over pairs of time-reversed paths; more complicated paths, such as represented by Hikami terms, are evidently not needed. (However, this simplification is somewhat fortuitous, since it occurs only when considering the unitary limit of the interaction propagator; for more general forms of the latter, the contribution of Hikami terms *is* essential, as emphasized by [16, 17].)

The fact that the standard result for $\gamma_\varphi$ *can* be reproduced from the influence functional approach is satisfying, since this approach is appealingly clear and simple, not only conceptually, but also for calculating $\gamma_\varphi$. Indeed, once the form of the influence functional (8.2) has been properly derived (wherein lies the hard

work), the calculation of $\langle i\tilde{S}_R + \tilde{S}_I\rangle_{\rm rw}$ requires little more than knowledge of the distribution function for a random walk and can be presented in just a few lines [Sec.4]; indeed, the algebra needed for the key steps [evaluating Eq. (8.7) to get the first terms of (8.10), then finding (8.10) and (8.17)] involves just a couple of pages.

We expect that the approach should be similarly useful for the calculation of other physical quantities governed by the long-time, low-frequency behavior of the Cooperon, provided that one can establish unambiguously that it suffices to include the contributions of time-reversed paths only — because Hikami-like terms, though derivable from the influence functional approach too, can not easily be evaluated in it; for the latter task, diagrammatic impurity averaging still seems to be the only reliable tool.

## Acknowledgments

I dedicate this paper to Vinay Ambegaokar on the occasion of his 70th birthday. He raised and sustained my interested in the present subject by telling me in 1998: "I believe GZ have a problem with detailed balance", which turned out to be right on the mark, in that recoil and detailed balance go hand in hand. I thank D. Golubev and A. Zaikin, and, in equal measure, I. Aleiner, B. Altshuler, M. Vavilov, I. Gornyi, R. Smith and F. Marquardt, for countless patient and constructive discussions, which taught me many details and subtleties of the influence functional and diagrammatic approaches, and without which I would never have been able to reach the conclusions presented above. I also acknowledge illuminating discussions with J. Imry, P. Kopietz, J. Kroha, S. Mirlin, H. Monien, A. Rosch, I. Smolyarenko, G. Schön, P. Wölfle and A. Zawadowski. Finally, I acknowledge the hospitality of the centers for theoretical physics in Trieste, Santa Barbara, Aspen and Dresden, where some of this work was performed.

## Appendix

Without dwelling on details of derivations, we outline in this appendix how the influence functional presented in Sec. 2 is derived. (A similar summary is contained in [14, 23]; however, it is incomplete, in that we have introduced important improvements since.) Before we start, let us point out the two main differences between our formulation and that of GZ:

(i) GZ formulated the Cooperon propagator in terms of a coordinate-momentum path integral $\int \mathcal{D}\boldsymbol{R}\int\mathcal{D}\boldsymbol{P}$, in which $(\tilde{\delta}-2\tilde{\rho}^0)$ is represented as $[1-2n_0(\tilde{h}_0)] = \tanh(\tilde{h}_0/2T)$, where the free-electron energy $\tilde{h}_0(\boldsymbol{R}(t_a),\boldsymbol{P}(t_a))$ depends on position and momentum. This formulation makes it difficult to treat the Pauli factor with sufficient accuracy to include recoil. In contrast, we achieve the latter by using a coordinates-only version $\int\widetilde{\mathcal{D}}'\boldsymbol{R}$, in which exact relations be-

tween noninteracting Green's functions make an accurate treatment of the Pauli factor possible, upon Fourier-transforming the effective action to the frequency domain.
(ii) GZ effectively performed thermal weighting at an initial time $t_0$ that is not sent to $-\infty$, but (in the notation of the main text) is set to $t_0 = -\tau/2$; with the latter choice, it is impossible to correctly reproduce the first (or higher) order terms of a perturbation expansion. GZ's claim [3] that they have reproduced these is incorrect (see end of App. C.3), since their time integrals have $-\tau/2$ as the lower limit, whereas in the Keldysh approach they run from $-\infty$ to $+\infty$. We have found that with some (but not much) extra effort it *is* possible to properly take the limit $t_0 \to -\infty$, to correctly recover the first order perturbation terms [App. C.3] and to express the conductivity in a form containing thermal weighting in the energy domain explicitly in the form of a factor $\int (d\varepsilon)[-n_0'(\hbar\varepsilon)]\tilde{P}^{\varepsilon}$, where $\tilde{P}^{\varepsilon}$ is an energy-dependent path integral, obtained by suitable Fourier transformation [App. B.6.3 and C.4].

## 1. Outline of derivation of influence functional

We consider a disordered system of interacting fermions, with Hamiltonian $\hat{H} = \hat{H}_0 + \hat{H}_i$:

$$\hat{H}_0 = \int dx\, \hat{\psi}^\dagger(x) h_0(x) \hat{\psi}(x)\ , \tag{8.A.1}$$

$$\hat{H}_i = \frac{e^2}{2}\int dx_1\, dx_2\ :\hat{\psi}^\dagger(x_1)\hat{\psi}(x_1): \tilde{V}_{12}^{\rm int} :\hat{\psi}^\dagger(x_2)\hat{\psi}(x_2):$$

Here $\int dx = \sum_\sigma \int d\boldsymbol{r}$, and $\hat{\psi}(x) \equiv \hat{\psi}(\boldsymbol{r},\sigma)$ is the electron field operator for creating a spin-$\sigma$ electron at position $\boldsymbol{r}$, with the following expansion in terms of the exact eigenfunctions $\psi_\lambda(x)$ of $h_0(x) = \frac{-\hbar^2}{2m}\boldsymbol{\nabla}_{\boldsymbol{r}}^2 + V_{\rm imp}(\boldsymbol{r}) - \mu$:

$$\hat{\psi}(x) = \sum_\lambda \psi_\lambda(x)\hat{c}_\lambda, \quad [h_0(x) - \xi_\lambda]\psi_\lambda(x) = 0. \tag{8.A.2}$$

The interaction potential $\tilde{V}_{12}^{\rm int} = \tilde{V}^{\rm int}(|\boldsymbol{r}_1 - \boldsymbol{r}_2|)$ acts between the normal-ordered densities at $\boldsymbol{r}_1$ and $\boldsymbol{r}_2$. The Kubo formula for the DC conductivity of a $d$-dimensional conductor gives

$$\sigma_{\rm DC} = -{\rm Re}\left[\lim_{\omega_0\to 0}\frac{1}{d\omega_0}\sum_{\sigma_1}\int dx_2\, \boldsymbol{j}_{11'}\cdot\boldsymbol{j}_{22'}\tilde{J}_{11',22}(\omega_0)\Big|_{x_1=x_{1'}}\right],$$

$$\tilde{J}_{11',22'}(\omega_0) = \int_{-\infty}^{\infty} dt_{12} e^{i\omega_0 t_{12}}\theta(t_{12})\,\tilde{C}_{[11',22']}\ , \tag{8.A.3}$$

$$\tilde{\mathcal{C}}_{[11',22']} \equiv \frac{1}{\hbar}\langle[\hat{\psi}^\dagger(t_1,x_{1'})\hat{\psi}(t_1,x_1),\hat{\psi}^\dagger(t_2,x_{2'})\hat{\psi}(t_2,x_2)]\rangle_H,$$

where $\boldsymbol{j}_{11'} \equiv \frac{-ie\hbar}{2m}(\boldsymbol{\nabla}_1 - \boldsymbol{\nabla}_{1'})$ and a uniform applied electric field $\boldsymbol{E}(\omega_0)$ was represented using uniform, time-dependent vector potential, $\boldsymbol{E}(\omega_0) = i\omega_0\boldsymbol{A}(\omega_0)$. A path integral representation for $\tilde{C}_{[11',22']}$ can be derived using the following strategy, adapted from GZ's Ref. [2]: (1) introduce a source term into the Hamiltonian, in which an artificial source field $\tilde{v}_{2'2}$ couples to $\hat{\psi}^\dagger(t_2,x_{2'})\hat{\psi}(t_2,x_2)$, and write $\tilde{C}_{[11',22']}$ as the linear response to the source field $\tilde{v}_{22'}$ of the single-particle density matrix $\tilde{\boldsymbol{\rho}}_{11'} = \langle\hat{\psi}^\dagger(t_1,x_{1'})\hat{\psi}(t_1,x_1)\rangle_H$. (2) Decouple the interaction using a Hubbard-Stratonovitch transformation, thereby introducing a functional integral over real scalar fields $V_{F/B}$, the so-called "interaction fields", defined on the forward and backward Keldysh contours, respectively; these then constitute a dynamic, dissipative environment with which the electrons interact. (3) Derive an equation of motion for $\tilde{\rho}^V_{11'}$, the single-particle density matrix for a given, fixed configuration of the fields $V_{F/B}$, and linearize it in $\tilde{v}_{2'2}$, to obtain an equation of motion for the linear response $\delta\tilde{\rho}^V_{11'}(t)$ to the source field. (4) Formally integrate this equation of motion by introducing a path integral $\int\widetilde{\mathcal{D}}'(\boldsymbol{R})$ over the coordinates of the single degree of freedom associated with the single-particle density matrix $\delta\tilde{\rho}^V_{11'}$. (5) Use the RPA-approximation to bring the effective action $S_V$ that governs the dynamics of the fields $V_{F/B}$ into a quadratic form. (6) Neglect the effect of the interaction on the single-particle density matrix whereever it occurs in the exponents occuring under the path integral $\int\widetilde{\mathcal{D}}'\boldsymbol{R}$, i.e. replace $\tilde{\rho}^V_{ij}$ there by the free single-particle density matrix

$$\tilde{\rho}^0_{ij} = \langle\hat{\psi}^\dagger(x_j)\hat{\psi}(x_i)\rangle_0 = \sum_\lambda \psi^*_\lambda(x_j)\psi_\lambda(x_i)\, n_0(\xi_\lambda)\ , \tag{8.A.4}$$

where thermal averaging is performed using $\langle\hat{O}\rangle_0 = \mathrm{Tr}e[^{-\beta\hat{H}_0}\hat{O}]/\mathrm{Tr}[e^{-\beta\hat{H}_0}]$. (7) Perform the functional integral (which steps (5) and (6) have rendered Gaussian) over the fields $V_{F/B}$; the environment is thereby integrated out, and its effects on the dynamics of the single particle are encoded in an influence functional of the form $e^{-(i\tilde{S}_R+\tilde{S}_I)}$. The final result of this strategy is that $\boldsymbol{j}_{22'}\cdot\boldsymbol{j}_{11'}\,\tilde{\mathcal{C}}_{[11',22']}$ can be written as [cf. (II.49)]

$$\int dx_2\,\boldsymbol{j}_{22'}\cdot\boldsymbol{j}_{11'}\tilde{\mathcal{C}}_{[11',22']} = \int dx_{0_F,\bar{0}_B}\,\tilde{\rho}^0_{0_F\bar{0}_B}\int_{0_F}^{1_F}\!\!\!\!\!\!\int_{\bar{0}_B}^{1'_B}\widetilde{\mathcal{D}}'(\boldsymbol{R}) \tag{8.A.5}$$
$$\times\,\frac{1}{\hbar}\Bigg\{\Big[\hat{\boldsymbol{j}}(t_{2_F})-\hat{\boldsymbol{j}}(t_{2_B})\Big]\hat{\boldsymbol{j}}(t_1)e^{-[i\tilde{S}_R+\tilde{S}_I](t_1,t_0)/\hbar}$$

where $\not\int\!\!\!\int \not\int\!\!\!\int \widetilde{\mathcal{D}}'(\boldsymbol{R})$ is used as a shorthand for the following forward and backward path integral between the specified initial and final coordinates and times:

$$\not\int_{j_F}^{i_F}\not\int\!\!\!\int_{\bar{\jmath}_B}^{\bar{\imath}_B}\widetilde{\mathcal{D}}'(\boldsymbol{R})\ldots \equiv \int_{\boldsymbol{R}^F(t_j^F)=\boldsymbol{r}_j^F}^{\boldsymbol{R}^F(t_i^F)=\boldsymbol{r}_i^F}\widetilde{\mathcal{D}}'\boldsymbol{R}^F(t_{3_F})\,e^{i\tilde{S}_0^F(t_i^F,t_j^F)/\hbar} \times \int_{\boldsymbol{R}^B(t_j^B)=\boldsymbol{r}_{\bar{\jmath}}^B}^{\boldsymbol{R}^B(t_i^B)=\boldsymbol{r}_{\bar{\imath}}^B}\widetilde{\mathcal{D}}'\boldsymbol{R}^B(t_{3_B})\,e^{-i\tilde{S}_0^B(t_i^B,t_j^B)/\hbar}\ldots \tag{8.A.6}$$

The complex weighting functional $e^{i(\tilde{S}_0^F-\tilde{S}_0^B)}$ occuring therein involves the action for a single, free electron. Expression (8.A.5) has a simple interpretation: thermal averaging with $\tilde{\rho}_{0\bar{0}}^0$ at time $t_0$ (for which we take the limit $\to -\infty$) is followed by propagation in the presence of interactions (described by $e^{-[i\tilde{S}_R+\tilde{S}_I]}$) from time $t_0$ up to time $t_1$, with insertions of current vertices $\hat{\boldsymbol{\jmath}}(t_{2_a})$ at time $t_2$ on either the upper or lower Keldysh contour.

For the purpose of calculating the Cooperon propagator, we now make the following approximation in Eq. (8.A.5) [referred to as "approximation (ii)" in App. B]: For the first or second terms, for which the current vertex occurs at time $t_{2_{\tilde{a}}}$ on contour $\tilde{a} = F$ or $B$ respectively, we neglect all interaction vertices that occur on the *same* contour $\tilde{a}$ at earlier times $t_{3_{\tilde{a}}}$ or $t_{4_{\tilde{a}}} \in [t_0, t_{2_{\tilde{a}}}]$; however, for the opposite contour containing no current vertex, we include interaction vertices for *all* times $\in [t_0, t_1]$, with $t_0 \to \infty$. [This turns out to be essential to obtain, after Fourier transforming, the proper thermal weighting factor $[-n_0'(\hbar\varepsilon)]$ occuring in Eq. (8.0), see App. C.3.] The rationale for this approximation is that, in diagrammatic language, this approximation retains only those diagrams for which *both* current vertices $\boldsymbol{\jmath}_{22'}$ and $\boldsymbol{\jmath}_{11'}$ are always sandwiched between a $\tilde{G}^R$- and a $\tilde{G}^A$-function; these are the ones relevant for the Cooperon. The contributions thereby neglected correspond to the so-called "interaction corrections". [If one so chooses, they latter *can* be kept track of, though.]

This approximation (ii) is much weaker than the one used by GZ at a similar point in their calculation: to simplify the thermal weighting factor describing the initial distribution of electrons, namely to obtain the explicit factor $\rho_0$ in Eq. (49) of [2], they set $t_0 \to t_2$ (their $t'$ corresponds to our $t_2$), and thereby perform thermal weighting at time $t_2$, instead of at $-\infty$. As a consequence, in their analysis all time integrals have $t_2$ as lower limit, which means that (contrary to their claims in [3]) they did not correctly reproduce the Keldysh first order perturbation expansion for $\tilde{\mathcal{C}}_{[11',22']}$, in which all time integrals run to $-\infty$. A detailed discussion of this matter is given in App. B.3. [Contrary to our initial expectations, but in agreement with those of GZ, it turns out, though,

that the choice of $t_0$ does not to have any implications for the calculation of $\tau_\varphi$, which does not to depend on whether one chooses $t_0 = t_2$ or sends it to $-\infty$.]

Having made the above approximation (ii), the effective action $(i\tilde{S}_R + \tilde{S}_I)$ occuring in Eq. (8.A.5) is found to have the following form (we use the notation $i\tilde{S}_R/\tilde{S}_I$ to write two equations with similar structure in one line, and upper or lower terms in curly brackets refer to the first or second case):

$$[i\tilde{S}_R/\tilde{S}_I](t_1,t_0) \equiv \sum_{aa'} \int_{t_0}^{t_1} dt_3 \int_{t_0}^{t_1} dt_4 \, (i\tilde{L}^R/\tilde{L}^I)_{3_a 4_{a'}} \,, \tag{8.A.7}$$

$$(i\tilde{L}^R/\tilde{L}^I)_{3_F 4_F} = -\tfrac{1}{2} i \;\theta_{34}\, \tilde{\delta}_{3_F \bar{3}_F} \left\{ \begin{matrix} [\tilde{\delta} - 2\tilde{\rho}^0]_{4_F \bar{4}_F} \\ \tilde{\delta}_{4_F \bar{4}_F} \end{matrix} \right\} \tilde{\mathcal{L}}^{R/K}_{\bar{3}_F \bar{4}_F} \,, \tag{8.A.8a}$$

$$(i\tilde{L}^R/\tilde{L}^I)_{3_B 4_F} = \quad \tfrac{1}{2} i \;\theta_{34} \left\{ \begin{matrix} [\tilde{\delta} - 2\tilde{\rho}^0]_{4_F \bar{4}_F} \\ \tilde{\delta}_{4_F \bar{4}_F} \end{matrix} \right\} \tilde{\mathcal{L}}^{R/K}_{\bar{3}_B \bar{4}_F} \, \tilde{\delta}_{\bar{3}_B 3_B} \,, \tag{8.A.8b}$$

$$(i\tilde{L}^R/\tilde{L}^I)_{3_F 4_B} = \mp \tfrac{1}{2} i \;\theta_{34}\, \tilde{\delta}_{3_F \bar{3}_F} \, \tilde{\mathcal{L}}^{A/K}_{\bar{4}_B \bar{3}_F} \left\{ \begin{matrix} [\tilde{\delta} - 2\tilde{\rho}^0]_{\bar{4}_B 4_B} \\ \tilde{\delta}_{\bar{4}_B 4_B} \end{matrix} \right\} , \tag{8.A.8c}$$

$$(i\tilde{L}^R/\tilde{L}^I)_{3_B 4_B} = \pm \tfrac{1}{2} i \;\theta_{34}\, \tilde{\mathcal{L}}^{A/K}_{\bar{4}_B \bar{3}_B} \, \tilde{\delta}_{\bar{3}_B 3_B} \left\{ \begin{matrix} [\tilde{\delta} - 2\tilde{\rho}^0]_{\bar{4}_B 4_B} \\ \tilde{\delta}_{\bar{4}_B 4_B} \end{matrix} \right\} . \tag{8.A.8d}$$

Here $\tilde{\delta}_{\bar{\imath} i} = \delta_{\sigma_{\bar{\imath}} \sigma_i} \delta(\boldsymbol{r}_{\bar{\imath}} - \boldsymbol{r}_i)$ and $(\tilde{\mathcal{L}}^{R,A,K})_{\bar{\imath}_a \bar{\jmath}_{a'}} = (\tilde{\mathcal{L}}^{R,A,K})\big(t_{i_a} - t_{j_{a'}}, \boldsymbol{r}^a_{\bar{\imath}}(t_{i_a}) - \boldsymbol{r}^{a'}_{\bar{\jmath}}(t_{j_{a'}})\big)$ are the standard retarded, advanced and Keldysh interaction propagators. For each occurrence in Eqs. (8.A.8) of a pair of indices, one without bar, one with, e.g. $4_a$ and $\bar{4}_a$, the corresponding coordinates $\boldsymbol{r}^a_4$ and $\boldsymbol{r}^a_{\bar{4}}$ are both associated with the *same* time $t_4$, and integrated over, $\int d\boldsymbol{r}^a_4 d\boldsymbol{r}^a_{\bar{4}}$, in the path integral $\int \mathcal{D}'(\boldsymbol{R})$. (This somewhat unusual aspect of the "coordinates-only" path integral used in our approach is discussed in explicit detail in App. D; it is needed to account for the fact that the density-matrix $\tilde{\rho}^0$ is non-local in space, and arises upon explicitly performing the $\int \mathcal{D}\boldsymbol{P}$ momentum path integral in GZ's formulation.) The $\tilde{\delta}_{\bar{\imath} i}$ functions on the right hand side of Eqs. (8.A.8) will kill one of these double coordinate integrations at time $t_i$.

Eqs. (8.A.7) and (8.A.8) are the main result of our rederivation of the influence functional approach. They are identical in structure (including signs and prefactors) to the corresponding expressions derived by GZ (Eqs. (68) and (69) of [2]), as can be verified by using the relations

$$-e^2 \tilde{R}_{\bar{\imath}\bar{\jmath}} = \tilde{\mathcal{L}}^R_{\bar{\imath}\bar{\jmath}} = \tilde{\mathcal{L}}^A_{j i}, \qquad e^2 \tilde{I}_{\bar{\imath}\bar{\jmath}} = e^2 \tilde{I}_{j i} = -\tfrac{1}{2} i \tilde{\mathcal{L}}^K_{\bar{\imath}\bar{\jmath}}, \tag{8.A.9}$$

to relate our interaction propagators $\tilde{\mathcal{L}}_{ij}$ to the functions $R_{ij}$ and $I_{ij}$ used by GZ. However, whereas Eqs. (68) and (69) of [2] are written in a mixed coordinate-momentum representation in which it is difficult to treat the Pauli factors $(\tilde{\delta} - 2\tilde{\rho}^0)$ sufficiently accurately, our expressions (8.A.8) are formulated in a coordinates-only version. Formally, the two representations are fully equivalent. The key advantage of the latter, though, is that passing to a coordinate-frequency representation (which can be done *before* disorder averaging, allows us to sort out the fate of $(\tilde{\delta} - 2\tilde{\rho}^0)$, as discussed in Sec. 3 [and extensively in App. B.6.3].

## 2. Cooperon self energy before disorder averaging

From the formalism outlined above, it is possible to recover the standard results of diagrammatic Keldysh perturbation theory, *before disorder averaging*, by expanding the path integral (8.A.5) in powers of the effective action $(i\tilde{S}_R + \tilde{S}_I)$. For example, using Eqs. (8.A.8) [and being sufficiently careful with signs, see App. B.6.1) one readily obtains the following expressions for Cooperon self energy $\tilde{\Sigma}^{R/I} = \sum_{aa'} \tilde{\Sigma}^{R/I}_{aa'}$ summarized diagrammatically in Fig. 8.A.1:

$$\left(\tilde{\Sigma}^{R/I}_{FF}\right)^{3_F\bar{4}_F}_{\bar{4}_B 3_B} = -\frac{i\hbar}{2}\,(\tilde{G}^{K/R})^{3_F\bar{4}_F}\tilde{G}^{A}_{\bar{4}_B 3_B}(\tilde{\mathcal{L}}^{R}/\tilde{\mathcal{L}}^{K})^{3_F\bar{4}_F}\,, \tag{8.A.10a}$$

$$\left(\tilde{\Sigma}^{R/I}_{BF}\right)^{3_F\bar{4}_F}_{\bar{4}_B 3_B} = -\frac{i\hbar}{2}\,(\tilde{G}^{K/R})^{3_F\bar{4}_F}\tilde{G}^{A}_{\bar{4}_B 3_B}(\tilde{\mathcal{L}}^{R}/\tfrac{1}{2}\tilde{\mathcal{L}}^{K})_{3_B}{}^{\bar{4}_F}, \tag{8.A.10b}$$

$$\left(\tilde{\Sigma}^{R/I}_{FB}\right)^{3_F\bar{4}_F}_{\bar{4}_B 3_B} = -\frac{i\hbar}{2}\,\tilde{G}^{R,3_F\bar{4}_F}(\tilde{G}^{K/A})_{\bar{4}_B 3_B}(\tilde{\mathcal{L}}^{A}/\tfrac{1}{2}\tilde{\mathcal{L}}^{K})_{\bar{4}_B}{}^{3_F}, \tag{8.A.10c}$$

$$\left(\tilde{\Sigma}^{R/I}_{BB}\right)^{3_F\bar{4}_F}_{\bar{4}_B 3_B} = -\frac{i\hbar}{2}\,\tilde{G}^{R,3_F\bar{4}_F}(\tilde{G}^{K/A})_{\bar{4}_B 3_B}(\tilde{\mathcal{L}}^{A}/\tilde{\mathcal{L}}^{K})_{\bar{4}_B 3_B}\,. \tag{8.A.10d}$$

To obtain this, we exploited the fact that every vertex occuring in the effective action is sandwidched between retarded propagators if it sits on the upper contour, and advanced ones on the lower contour. The Keldysh functions arise from using some exact identities, valid (before impurity averaging) in the coordinate-time representation: depending on whether a vertex at time $t_{4'_a}$ sits on the forward (time-ordered) or backward (anti-time-ordered) contour ($a' = F/B$), the factor $(\tilde{\delta} - 2\tilde{\rho}^0)\tilde{\mathcal{L}}^{R/A}$ occuring in $\tilde{L}^{R}_{aa'}$ is sandwidched as follows (on the left hand sides below, a coordinate integration $\int dx_{4_{a'}}$ over the un-barred variable at vertex 4 is implied):

$$\left[\tilde{G}^{R}_{i_F 4_F}(\tilde{\delta} - 2\tilde{\rho}^0)_{4_F\bar{4}_F}\right]\tilde{\mathcal{L}}^{R}_{3\bar{4}_F}\,\tilde{G}^{R}_{\bar{4}_F j_F} \quad\rightarrow\quad \tilde{G}^{K}_{i_F\bar{4}_F}(\bar{\varepsilon} - \bar{\omega})\,\tilde{\mathcal{L}}^{R}_{3\bar{4}_F}(\bar{\omega})\,\tilde{G}^{R}_{\bar{4}_F j_F}(\bar{\varepsilon}), \tag{8.A.11a}$$

$$\tilde{G}^{A}_{\bar{j}_B\bar{4}_B}\,\tilde{\mathcal{L}}^{A}_{\bar{4}_B 3}\left[(\tilde{\delta} - 2\tilde{\rho}^0)_{\bar{4}_B 4_B}\tilde{G}^{A}_{4_B\bar{i}_B}\right] \quad\rightarrow\quad -\tilde{G}^{A}_{\bar{j}_B\bar{4}_B}(\bar{\varepsilon})\,\tilde{\mathcal{L}}^{A}_{\bar{4}_B 3}(\bar{\omega})\,\tilde{G}^{K}_{4_B\bar{i}_B}(\bar{\varepsilon} - \bar{\omega}) \tag{8.A.11b}$$

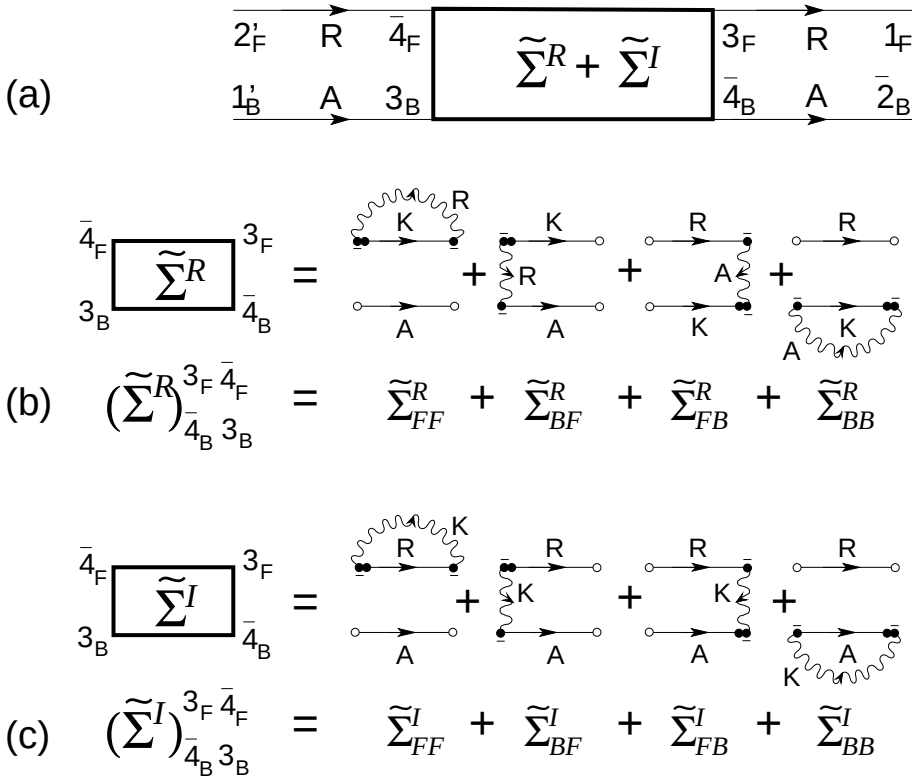


*Figure 8.A.1.* First order contributions to the irreducible self energy of the Cooperon, illustrating Eqs. (8.A.10). The arrows associated with each factor $\tilde{G}_{ij}$ or $\tilde{\mathcal{L}}_{ij}$ in Eqs. (8.A.10) are drawn to point from the second index to the first ($j$ to $i$). Filled double dots denote the occurence of a factor $(\tilde{\delta} - 2\tilde{\rho})_{4_F\bar{4}_F}$ on the upper contour or $(\tilde{\delta} - 2\tilde{\rho})_{\bar{4}_B 4_B}$ on the lower contour. Bars on filled dots are used to indicate the barred indices to which the interaction lines is connected. Both filled and open single dots indicate a delta function $\tilde{\delta}$; the open dots stand for delta functions that have been inserted to exhaust dummy integrations, as discussed after Eqs. (8.A.8). The diagrams in (b) and (c) coincide precisely with the those obtained by standard Keldysh diagrammatic perturbation theory for the Cooperon self energy, as depicted, e.g., in Fig. 2 of Ref. [17]. (There, impurity lines needed for impurity averaging are also depicted; the present figure, impurity averaging has not yet been performed.)

The left- and right-hand sides are written in the time and frequency domains, respectively. To obtain Keldysh functions from the left-hand side expressions, we exploit the fact that the upper or lower contours are time- or anti-time-ordered to add an extra $-\tilde{G}^{A/R} = 0$, and then exploited Eqs. (8.5a) to obtain a factor $\pm\tilde{G}^K$.

## 3. Thermal averaging

It remains to figure out how the thermal weighting in the first line of Fig. 8.0 can be derived from our general path integral expression Eq. (8.A.5). This is a standard, if nontrivial, excercise in Fourier transformation, carried out (along the lines of a similar analysis by AAK [9]) in App. B.6.4 and C.4. The result is an equation for the conductivity similar to Eq. (8.A.5), but with a more complicated path integral, given by

$$\tilde{P}_{43}^{12,\varepsilon}(\tau_{12}) = \int_{-\infty}^{\infty} d\widetilde{\tau}_{12} \int (d\widetilde{\omega})\, e^{i\widetilde{\omega}\widetilde{\tau}_{12}} \int_{-\infty}^{\infty} d\bar{\tau}_{12} e^{i\bar{\tau}_{12}(\varepsilon - \frac{1}{2}\widetilde{\omega})} \tilde{P}_{43}^{12} \ . \quad \text{(8.A.12)}$$

Here the notation $P_{34}^{12}$ is used as a shorthand for the general double path integral

$$\tilde{P}_{43}^{12} \equiv \theta_{12} \int\!\!\!\!\!\!\int_{\boldsymbol{R}^F(t_2^F)=\boldsymbol{r}_2^F}^{\boldsymbol{R}^F(t_1^F)=\boldsymbol{r}_1^F} \int\!\!\!\!\!\!\int_{\boldsymbol{R}^B(t_4^B)=\boldsymbol{r}_4^B}^{\boldsymbol{R}^B(t_3^B)=\boldsymbol{r}_3^B} \widetilde{\mathcal{D}}'(\boldsymbol{R})\, e^{-[i\tilde{S}_R + \tilde{S}_I]/\hbar} \ , \qquad \text{(8.A.13)}$$

ranging from time $t_2^F$ to $t_1^F$ on the forward contour (to be called "forward piece") and from $t_4^B$ to $t_3^B$ on the backward contour (to be called "backward piece"), and the time integration variables in Eq. (8.A.12) are defined as follows:

$$\begin{aligned} &\tau_{12} = \tfrac{1}{2}\big[(t_1^F - t_2^F) + (t_3^B - t_4^B)\big], \quad \widetilde{\tau}_{12} = \tfrac{1}{4}\big[(t_1^F + t_2^F) - (t_3^B + t_4^B)\big], \\ &\bar{\tau}_{12} = (t_1^F - t_2^F) - (t_3^B - t_4^B) \ . \end{aligned} \qquad \text{(8.A.14)}$$

[The notation for $\tilde{P}_{21'}^{12',\varepsilon}(\tau_{12})$ takes it to be understood that the indices $(12', 21')$ refer only to position coordinates, whereas the time arguments $t_1^F$, $t_2^F$, $t_3^B$, $t_4^B$ are as indicated in Eq. (8.A.13), and are converted to $\tau_{12}$, $\widetilde{\tau}_{12}$ and $\bar{\tau}_{12}$ via Eq. (8.A.14).]

We need to consider $\big\langle \tilde{P}_{21'}^{12'} \big\rangle_{\text{dis}}$ only in the limit $\boldsymbol{r}_2 \to \boldsymbol{r}_1$, since the Cooperon contribution to it decays as $e^{-|\boldsymbol{r}_2 - \boldsymbol{r}_1|/l_{\text{el}}}$, where $l_{\text{el}}$ is the elastic scattering length. The purpose of the time integrals in Eq. (8.A.12) is to project out from the general path integral $P_{34}^{12}$, defined in the position-time domain, an object depending in an appropriate way on the energy $\varepsilon$ occuring in the thermal weighting factor: The $\int d\widetilde{\tau}_{12}$ integral fixes the average energy of the upper and lower electron lines (in diagrammatic language) to be $\varepsilon - \widetilde{\omega}/2$ [where $\widetilde{\tau}_{12}$ is the length difference between the forward and backward pieces of the contour]. The $\int (d\widetilde{\omega})$ integral averages over all possible frequency differences $\widetilde{\omega}$ between the upper and lower

electron lines, as is necessary when vertex terms are present that transfer energy between them. And finally, the $\int d\widetilde{\tau}_{12}$ integral projects out the $\widetilde{\tau}_{12}$-dependence of $P_{43}^{12}$ [where $\widetilde{\tau}_{12}$ is the difference between the midpoints of the forward and backward pieces of the contour]. The only remaining time variable, $\tau_{12}$, is the average of the lengths of the forward and backward pieces, and can be viewed as the "observation time" as a function of which $\tilde{P}_{21'}^{12',\varepsilon}(\tau_{12})$ will decay. $\tilde{P}_{21'}^{12',\varepsilon}(\tau_{12})$ will contain a contribution resulting from time-reversed paths that corresponds to the full Cooperon in the position-time representation, $\tilde{C}_{\boldsymbol{\rho}=0}(\tau_{12})$. The time scale on which it decays is the desired decoherence time $\tau_\varphi$.

Now, to properly and dutifully perform the integrals in Eq. (8.A.12) would be an unfeasibly complicated task in the path integral approach. (Diagrammatically, too, this is difficult, as will be discussed in [19].) To avoid these complications, we shall use a rather rough but effective shortcut [used by GZ too, but not explicitly discussed as such, since they chose not to discuss thermal averaging as explicitly as in Eqs. (8.0)]: to extract from $\tilde{P}_{21'}^{12'}$ an object depending only on the time $\tau_{12}$, we simply set $\widetilde{\tau}_{12}=0$, $\bar{\tau}_{12}=0$ and $\widetilde{\omega}=0$, instead of integrating them out, assuming that this will not too strongly affect the resulting $\tau_{12}$-dependence of $\tilde{P}_{43}^{12,\varepsilon}(\tau_{12})$. (The merits of this approximation will be discussed in more detail elsewhere [19].) Thus, we set $t_1^F=t_3^F=\tau/2$ and $t_2^F=t_4^B=-\tau/2$, which implies that the observation time is $\tau_{12}=\tau$. The result is that we $\tilde{P}_{43}^{12,\varepsilon}(\tau_{12})$ by the object $\tilde{P}_{21',\mathrm{eff}}^{12',\varepsilon}(\tau)$ defined in Eq. (8.1). When doing so, we should choose the energy variable $\hbar\varepsilon$ occuring in the $\tanh[\hbar(\varepsilon-\bar{\omega})/2T]$-factor of $\tilde{S}_R$ to be the same as that occuring in the thermal weighting factor $[-n_0'(\hbar\varepsilon)]$. In diagrammatic terms this approximation is rather natural: it corresponds to fixing the average energy of the upper and lower electron lines to be $\varepsilon$.

## References


[1] D. S. Golubev and A. D. Zaikin, Phys. Rev. Lett. **81**, 1074, (1998).

[2] D. S. Golubev and A. D. Zaikin, Phys. Rev. B **59**, 9195, (1999).

[3] D. S. Golubev and A. D. Zaikin, Phys. Rev. B **62**, 114061 (2000).

[4] D. S. Golubev, A. D. Zaikin, and G. Schön, J. Low Temp. Phys. 126, 1355 (2002) [cond-mat/0110495].

[5] D. S. Golubev and A. D. Zaikin, cond-mat/0208140.

[6] D. S. Golubev, C. P. Herrero, Andrei D. Zaikin, cond-mat/0205549.

[7] P. Mohanty, E. M. Q. Jariwala, and R. A. Webb, Phys. Rev. Lett. **78**, 3366 (1997); Fortschr. Phys. **46**, 779 (1998).

[8] Most relevant references can be found in Ref. [4], which gives a useful overview of the controversy from GZ's point of view.

[9] B. L. Altshuler, A. G. Aronov, and D. E. Khmelnitskii, J. Phys. C **15**, 7367 (1982).

[10] K. A. Eriksen and P. Hedegard, cond-mat/9810297; GZ replied in cond-mat/9810368.

[11] M. Vavilov and V. Ambegaokar, cond-mat/9902127.

[12] T.R. Kirkpatrick, D. Belitz, cond-mat/0112063, cond-mat/0111398.

[13] Y. Imry, cond-mat/0202044.

[14] J. von Delft, J. Phys. Soc. Jpn. Vol. 72 (2003) Suppl. A pp. 24-29 [cond-mat/0210644].

[15] F. Marquardt, cond-mat/0207692 (unpublished).

[16] I. Aleiner, B. L. Altshuler, and M. E. Gershenzon, Waves and Random Media **9**, 201 (1999) [cond-mat/9808053]; Phys. Rev. Lett. **82**, 3190 (1999).

[17] I. L. Aleiner, B. L. Altshuler, M. G. Vavilov, J. Low Temp. Phys. 126, 1377 (2002) [cond-mat/0110545].

[18] I. L. Aleiner, B. L. Altshuler, M. G. Vavilov, cond-mat/0208264.

[19] F. Marquardt, Jan von Delft, R. Smith and V. Ambegaokar, to be published.

[20] The appendices referred to in this paper will be published separately and posted on the cond-mat preprint server. They can also be obtained from the author by request.

[21] S. Chakravarty and A. Schmid, Phys. Rep. **140**, 193 (1983).

[22] H. Fukuyama and E. Abrahams, Phys. Ref. B **27**, 5976 (1983).

[23] The expressions for $\tilde{\Sigma}$ that we published in [14], Eqs. (A.16), contain incorrect signs and missing factors of $\frac{1}{2}$, and should be replaced by Eqs. (8.A.10) of this paper.